BMB
Reports

Molecular docking study on the α3β2 neuronal nicotinic acetylcholine receptor complexed with α-Conotoxin GIC

Chewook Lee[1], Si-Hyung Lee[1], Do-Hyoung Kim[1] & Kyou-Hoon Han[1,2,]*

[1]Biomedical Translational Research Center, Korea Research Institute of Bioscience and Biotechnology, Daejeon 305-806, [2]Department of Bioinformatics, University of Science and Technology, Daejeon 305-333, Korea

Nicotinic acetylcholine receptors (nAChRs) are a diverse family of homo- or heteropentameric ligand-gated ion channels. Understanding the physiological role of each nAChR subtype and the key residues responsible for normal and pathological states is important. α-Conotoxin neuropeptides are highly selective probes capable of discriminating different subtypes of nAChRs. In this study, we performed homology modeling to generate the neuronal α3, β2 and β4 subunits using the x-ray structure of the α1 subunit as a template. The structures of the extracellular domains containing ligand binding sites in the α3β2 and α3β4 nAChR subtypes were constructed using MD simulations and ligand docking processes in their free and ligand-bound states using α-conotoxin GIC, which exhibited the highest α3β2 vs. α3β4 discrimination ratio. The results provide a reasonable structural basis for such a discriminatory ability, supporting the idea that the present strategy can be used for future investigations on nAChR-ligand complexes. [BMB Reports 2012; 45(5): 275-280]

INTRODUCTION

Nicotinic acetylcholine receptors (nAChRs) are ligand-gated ion channels found in the neuromuscular junction, and the peripheral and central nervous systems of both invertebrates and vertebrates. nAChRs can be activated by the endogenous neurotransmitter acetylcholine or the tobacco plant toxin, nicotine, and play essential roles in regulating synaptic transmission signal (1-3). nAChRs form many different molecular subtypes. For example, some neuronal subtypes are comprised of homopentameric arrangements of identical subunits, $(\alpha 7)_5$ and $(\alpha 9)_5$, whereas others have heteropentameric compositions such as

*Corresponding author. Tel: +82-42-860-4250; Fax: +82-42-860-4259; E-mail: khhan600@kribb.re.kr

$(\alpha 1)_2\beta 1\gamma\delta$, $(\alpha 3)_2(\beta 2)_3$, and $(\alpha 4)_2(\beta 2)_3$. Such different receptor subtypes possess discrete anatomical locations and are associated with various physiological functions. Dysfunction or dysregulation of nAChRs has been implicated in a variety of neuropsychiatric disease states including schizophrenia, Parkinson, Alzheimer, depression, and nicotine addiction (1). Several drug discovery programs are aimed at developing neuromodulators that selectively act on specific subtypes of nAChRs (3). However, functional and structural differentiation among different nAChR subtypes is a daunting task due to the similarities in the amino acid sequences of individual nAChR subunits and in the overall topology of all nAChR subtypes.

The venom of *Conus* (marine snail) contains hundreds of neurotoxic peptides that are notable for their small size, potency, and subtype selectivity towards various ion channels (4). One of the most common types of *Conus* peptides is the α-conotoxin family that acts at the nAChR subtypes such as singlet α7 (5); doublet α3β2 (6), α3β4 (7), α4β2 (8), and α9α10 (9); triplet α1β1δ (10), α3α7β4 (11), and α6β2β3 (12); and quartet α1β1γδ (8) and α1β1εδ (13) subunit combinations. Alpha-conotoxins are typically composed of fewer than 20 amino acid residues and are compact molecules, as they contain two disulfide bridges. These neuropeptide have been extremely valuable in revealing the anatomical locations of certain nAChR subtypes. Extensive structural characterization and comparison of several α-conotoxins suggested residues that might be important for their subtype recognition specificities Table 1(14-20). In particular, the structural studies on the α4/7-conotoxins have shown that these toxins with a same "ω-shaped" backbone topology can display a widely different receptor recognition profiles by relying on subtle differences in their surface properties (14, 15, 19, 21). Above all, the precise delineation of contact sites that are responsible for specific recognition between a particular receptor subtype and its ligands requires high-resolution structures of the complexes of many receptor subtypes with various ligands displaying a large window of affinities. Unfortunately, only limited information acquired by x-ray and nuclear magnetic resonance (NMR) methods is available (22-25).

Topologically, nAChRs are composed of five identical or different subunits arranged around the 5-fold pseudo-symmetrical main axis oriented perpendicular to the cell membrane (1). The ligand-binding sites in nAChR are located at the interface be-

tween the extracellular domains (ECDs) of two subunits (e.g., α1γ and α1δ subunit interfaces in the case of the muscular nAChR, and α3β2, α3β4, or α4β2 subunit interfaces in the case of the neuronal nAChRs). Since understanding the detailed ligand-receptor contact sites for nAChRs at an atomic resolution is extremely useful, not only for better understanding of the ligand binding mechanism but also for designing potential nAChR-specific neuromodulators, several investigators have tried to experimentally determine the three-dimensional structures of the ECDs from different nAChR subunits. These efforts failed due to the poor solubility of the expressed ECDs (26). However, an x-ray structure of AChBP (PDB ID: 1I9B), a soluble homolog of nAChR ECD found in in-land snails, became available about a decade ago (22). This publication opened an alternative way for obtaining structural information of ECDs by harnessing *in silico* methods such as homology modeling, molecular dynamics, and ligand docking. Various homology modeled structures of nAChR ECD based on this AChBP structure have been generated and have proven useful in providing reliable knowledge on the high-resolution topology of the pentameric arrangements of nAChR subunits and the potential receptor-bound modes of sev-

eral ligands (2, 25). One drawback of these AChBP-based homology modeled structures has been the limited accuracy of such structures in providing an unambiguous understanding of the ligand binding mechanism of nAChRs and for designing potential neuromodulators, since they are obtained by homology modeling procedures using low sequence homology (only ~25%) between AChBP and nAChR subunits. More recently, the x-ray structure of the ECD from mouse α1 subunit (PDB ID: 2QC1), whose sequence homology with human nAChR subunits is much higher (≥50%), became available (24), which has provided a more reliable platform for generation of better homology models of ECDs.

α-Conotoxin GIC (denoted as GIC) is a 16-residue peptide isolated from the venom of the cone snail *Conus geographus* (6). This toxin potently blocks the α3β2 subtype of human nAChR, showing the highest known selectivity (100,000-fold selective for the α3β2 subtype vs. the muscle receptor of nCAhR) for neuronal versus muscle subtype of any nicotinic ligand characterized to date. Interestingly, GIC exhibits a high affinity (~1 nM) to the α3β2 receptor subtype, but a much lower (~700-fold) affinity towards the α3β4 subtype, thus is able to differentiate two close-

Table 1. Sequences and nAChR recognition profiles of 5 α-conotoxin subfamilies

Name[a]	Sequence[b]	Specificity
α3/5 sub-family[c]		
GI	E**CC** NPA**C** GRHYS **C***	α1/γ
MI	GR**CC** HPA**C** GKNYS **C***	α1/γ
SI	I**CC** NPA**C** GPKYS **C***	None
SIA	Y**CC** HPA**C** GKNFD **C***	α1/γ
CnIA	GR**CC** HPA**C** GKYYS **C***	α1/γ, α1/δ
CnIB	**CC** HPA**C** GKYYS **C***	α1/γ, α1/δ
α4/3 sub-family		
ImI	G**CC** SDPR**C** AWR **C***	α3/β2 > α7 > α3/β4
ImII	A**CC** SDRR**C** RWR **C***	α7≅α1/δ, α1/ε > α3/β2
α4/4 sub-family		
BuIA	G**CC** STPP**C** AVLY **C***	α6/β2 > α6/β4 ≅ α3β2 > α3/β4 ≅ α4/β4 > α2/β4 ≅ α7
α4/6 sub-family		
AuIB	G**CC**SYPP**C**FATNPD **C***	α3/β4
α4/7 sub-family		
EI[c]	RDO**CC**YHPT**C**NMSNPQI**C***	α1/δ
MII	G**CC**SNPV**C**HLEHSNL**C***	α6/β2≅α3/β2 > α4/β2 ≅ α3/β4
PnIA	G**CC**SLPP**C**AANNPDY**C***	α3/β2 > α7 > α3/β4
PnIB	G**CC**SLPP**C**ALSNPDY**C***	α7 > α3/β2
AuIA	G**CC**SYPP**C**FATNSDY**C***	α3/β4
AuIC	G**CC**SYPP**C**FATNSGY**C***	α3/β4
EpI	G**CC**SDPR**C**NMNNPDY**C***	α3/β2 ≅α3/β4
GID[d]	IRDr **CC**SNPA**C**RVNNOHV**C***	α3/β2 ≅ α7 > α4/β2
GIC	G**CC**SHPA**C**AGNNQHI**C***	α3/β2 ≅ α6/β2 > α4/β2 ≅ α3/β4
PIA	RDP**CC**SNPV**C**TVHNPQI**C***	α6/β2 > α6/β4≅α3/β2 > α3/β4
OmIA	G**CC**SHPA**C**NVNNPHI**C**G*	α4/β2

[a]The first capital letter indicates the species origin. [b]The asterisk indicates an amidated C-terminus. [c]For the α3/5 sub-family and α-conotoxin EI the specificity is for *Torpedo* receptor. [d]γ, γ-carboxyglutamic acid; O, γ-hydroxyproline.

ly-related neuronal nAChR subtypes. Little is known at a structural level as to how GIC can exhibit differential binding affinities towards two different neuronal nAChR subtypes. Here, we explored a combined *in silico* method (homology modeling, molecular dynamics simulations, and docking) to understand the structural basis for such a huge receptor subtype discriminatory ability of GIC.

RESULTS AND DISCUSSION

For a few decades, an important issue in the nAChR field has been how to obtain detailed information about ligand-nAChR interactions in the absence of high-resolution three-dimensional structures of ligand-nAChR complexes. Two alternative strategies have been used to study the mechanism of ligand-nAChR interactions. The first is to delineate receptor residues that might interact with ligands through receptor modification by chemical or biochemical means. Several potential ligand-binding residues have been suggested from studies using mutant receptors and affinity labeled receptors (27-30). Ligand binding modes of these residues have been confirmed in recent homology modeled structures of nAChRs (31) and the x-ray structures of AChBP bound to α-conotoxins (23, 25, 32) or α-cobratoxin (33). Another strategy for studying nAChR-ligand interactions has been to identify potential receptor-binding pharmacophores within various ligands including α-conotoxins (16, 17, 19, 21, 34-37). Here, we have generated high-resolution structures of ligand-nAChR complexes using α-conotoxin GIC, a well-known antagonistic ligand of nAChRs, and the extracellular domains of nAChRs that are homology modeled using the α1 subunit of mouse, which has much higher sequence homology with nAChR subunits than acetylcholine binding protein (AChBP).

### Homology modeling of individual subunits of human nAChRs
The three-dimensional structures of individual human nAChR subunits (α3, β2, and β4) were obtained by homology modeling procedure using MODELLER v9.8 (38) taking the x-ray structure of mouse α1 subunit as a template. The amino acid sequence of the human α1 subunit aligned by the LALIGN program (39) revealed a high sequence homology (95.2%) to that of mouse α1 (Table 2). Calculated Cα root mean square deviation (RMSD) between the mouse α1 and human α1 homology modeled ECD structures is 0.458 Å, indicating that the human α1 ECD structure is essentially

Table 2. Sequence homology between human and mouse nAChR subunits (unit: %)

	Mouse α1	Human α1	Human α3	Human β2	Human β4
Mouse α1	100				
Human α1	95.2	100			
Human α3	51.9	50.2	100		
Human β2	43.4	42.4	48.8	100	
Human β4	41.4	41.6	48.1	70.4	100

the same as that of the mouse α1 subunit. Sequence homology among the human α3, β2, and β4 subunits to the mouse α1 subunit was 51.9%, 43.4%, and 41.4%, respectively. These values were well above the "twilight zone" (i.e., sequence homology of <30%), suggesting the homology modeled ECD structures of these subunits obtained from the mouse α1 subunit template should be reliable. Indeed, Cα RMSDs of the human α3, β2, and β4 ECD structures compared with the x-ray structure of mouse α1 ECD were 0.682 Å, 0.205 Å, and 0.258 Å, respectively, confirming that the ECD structures of three subunits were reasonably modeled.

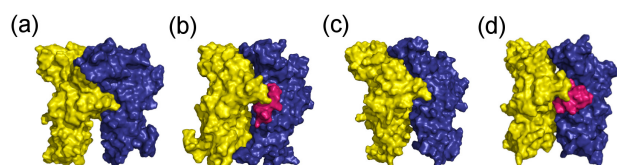### Conformational properties of pentameric nAChRs
The initial pentameric molecular topology for the α3β2 and α3β4 pentameric nAChR subtypes was inferred from the crystal structure of the α7 homopentameric of AChBP (PDB ID: 2C9T) in complex with α-conotoxin ImI (25). To form the heteropentameric structures, two α3 subunits and three β subunits (β2 or β4) were substituted into the positions of the α7 subunits at the beginning of the MD simulations. Due to differences in the length and the amino acid composition of each subunit, the structures of the α3β2 pentamer and the α3β4 pentamer differed slightly from that of the α7 pentamer. For example, as shown in Fig. 1A-1C, the bottom portions of the ECD in the α3β2 and α3β4 pentamers were slightly wider than that in the α7
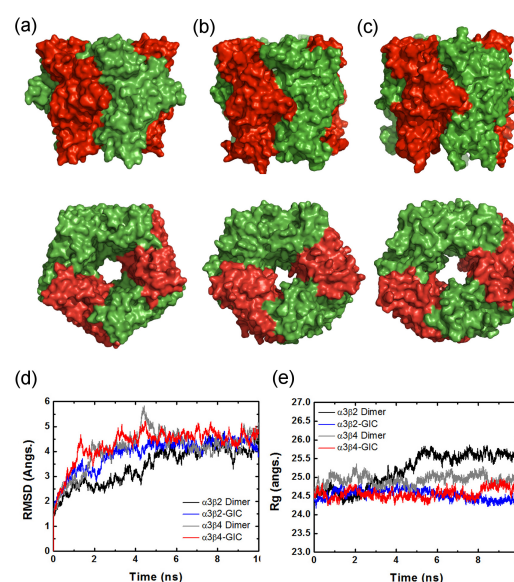
Fig. 1. Structures of three pentameric nAChR subtypes (a) (α7)$_5$ extracted from PDB 2C9T, (b) (α3)$_2$(β2)$_3$, and (c) (α3)$_2$(β4)$_3$ obtained by 10 ns MD simulations (top panel: side-view, middle panel: top-view). The α7 subunits in (a) are presented in red and green. All α3 subunits in (b) and (c) are shown in red and β2 and β4 subunits in green. Cα RMSD (d) and radius of gyration (e) of α3β2 dimer (black), α3β2-GIC complex (blue), α3β4 dimer (gray), and α3β4-GIC complex (red) from the initial structures as a function of simulation time at 300K under the TIP3P explicit water condition.
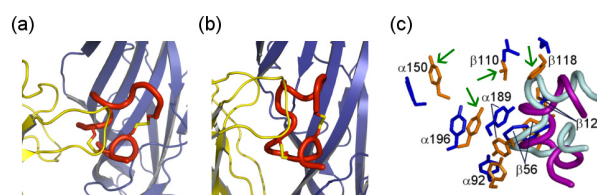
Fig. 2. The space-filling model structures of the dimer interfaces with and without GIC. Panels (a-d) depict α3β2 dimer, α3β2-GIC complex, α3β4 dimer, and α3β4-GIC complex, respectively. The α3 subunit is shown in yellow, β subunits (β2 and β4) are shown in blue, and GIC is shown in pink.

Fig. 3. Cartoon representations of the docked GIC after 10 ns MD simulations into (a) α3β2 and (b) α3β4 subunit interfaces. The principal subunit α3 is shown in yellow and the complementary subunits (β2 and β4) are shown in blue. GIC is shown in red. The yellow stick within GIC indicates two disulfide bridges. Note that the C-loop (cholinergic receptor region) of the principal subunit partly wraps up the toxin. (c) Superposition of the key ligand-binding residues in the principal subunit (α3) and the complementary subunits (β2 and β4). The residues at the α3β2 and at the α3β4 subunit interface are shown in orange and blue, respectively. GIC at the former is represented as a purple rod, whereas that at the latter is shown as a cyan rod. The green arrows point to the main differences between two subtypes interacting with GIC. (α3 subunit: Y92, Y150, Y189, Y196 / β2 subunit: W56, V110, F118, L120 / β4 subunit: W56, I110, L118, L120).

pentamer. Nevertheless, the pentameric topology of the α3β2 or α3β4 subtypes was well-preserved during the simulation, as evidenced by the Cα RMSD and radius of gyration, Rg (Fig. 1D and 1E). In particular, the subunit interfaces were well modeled, so that the C-loop region (or the cholinergic receptor fragment, CRF) in the α3 subunit that contains the major sites for ligand binding was properly positioned for ligand binding.

Ligand docking and MD simulations of the dimeric interfaces

The heteropentameric nAChR subtypes with a composition of $(\alpha m)_2(\beta n)_3$ have two equivalent ligand binding sites at their αm-βn subunit interfaces. Thus, to reduce computational costs, we modeled only the dimeric αm-βn subunit interfaces, rather than performing MD calculations for the entire pentameric structure. The α3β2 and α3β4 dimers were generated by MD simulations at 300K under explicit solvent water molecules. The MD simulation results consisted of two parts: with and without GIC ligand. Each simulation was done for the two subtype interfaces: one for the α3β2 interface and the other for the α3β4. The four resulting structures are shown in Fig. 2. Average RMSD values from initial dimer structures during the last 5 ns were 4.04 (±0.23) Å and 4.40 (±0.29) Å for the α3β2 dimer and the α3β4 dimer, respectively. The overall dimension of these structures could be estimated from their Rg values (Fig. 1E). The size of the α3β2 dimer was larger than that of the α3β4 dimer (black and grey lines), mostly due to the size differences between the interfaces of α and β subunit. The C-loop cholinergic fragments located in the central region of both dimers were of similar size.

The final structures of MD simulation and ligand docking showing the details of individual residues involved in ligand binding are shown in Fig. 3A and 3B. As described above, all the structures were fairly stable and the structural variations were quite small after 5 ns of MD simulations (Fig. 1D and 1E). The β-strands composing two inner and outer β-sheets in each subunit were well preserved, as was the overall structure of GIC. Rg value of the α3β2-GIC and α3β4-GIC complex was 6.62 ± 0.10 Å and 6.49 ± 0.11 Å, respectively. The overall binding position in the interface and the orientation of the key hydrophobic side-chains of GIC were fairly well positioned in the hydrophobic pocket of the nAChR subunits. Such a disposition of ligands has been reported for other α-conotoxins (23, 40, 41). GIC displays an affinity that was ∼700-fold higher to the α3β2

receptor subtype ($IC_{50} = 1.1$ nM) than to the α3β4 subtype ($IC_{50} = 755$ nM) (6). Fig. 3C explains how such a difference may manifest on a structural level. For the α3β2 subtype, GIC can have favorable hydrophobic contacts. The side-chains of α150Y, α196Y, β110V, and β118F in the α3β2 subtype are more closely located to the ligand than the side-chains of the corresponding residues in the α3β4 subtype. For example, the residual distance during the last 5 ns of simulation between α196Y and β118F in the α3β2-GIC subtype (8.57 ± 0.53 Å) was much closer than that of between α196Y and β118L in α3β4-GIC subtype (17.36 ± 0.49 Å). Also, the averaged center of mass distance between Tyr196 of α subunit and Cys8 of GIC in the α3β2-GIC and α3β4-GIC complex was 10.29 ± 0.55 and 11.05 ± 0.64 Å, respectively. In addition the number of hydrophobic residual contacts between the α3β2 subtype and GIC were larger (19.8 ± 2.5) than those found between the α3β4 subtype and GIC (14.6 ± 2.4) during the last 5 ns of MD simulation. Cys191 and Cys192 in the C-loop of α-subunit in the α3β2 subtype strongly interacted with Cys8, Ile15, and Cys16 of GIC (averaged population 64%, < 9.0 Å of center of mass distance) and those in the α3β4 subunit interacted with Cys2, Cys8, and Ala9 of GIC (60%) during last 5 ns of MD simulation. Therefore, the C-loop in α-subunit plays an important role of hydrophobic interaction with GIC. Also, Leu120 of the β-subunit in α3β2 interacted with Ala7 and Ala9 of GIC (averaged population 96%) and Leu168 interacted with Cys3 and Ala9 (99% and 64%, respectively). In the case of α3β4, Leu57 and Leu120 of the β-subunit interacted with Ala9 of GIC (99% and 73%, respectively). Besides these strong hydrophobic interactions, many medium and weak interactions were observed. These interactions are very influential to the binding affinity. Therefore, binding affinity differences are related with the residual contact around the ligand GIC.

In this work, we performed homology modeling of human α

and β subunits and MD simulation on the dimers and pentamers of nAChRs with and without GIC. Homology modeled ECD structures of human nAChR subunits highly resembled the experimentally-determined structure of the mouse nAChR α1 subunit and were used as an input for molecular dynamics simulation to build the pentameric ECD domains in the $(α3)_2(β2)_3$, and $(α3)_2(β4)_3$ nAChR subtypes. The difference in binding affinity of GIC towards the two subtypes was fairly well explained in terms of the orientation of the side-chains in the α3 and β2/β4 subunits. Our results suggest that the *in silico* approach we have used here is a promising tool for studying other nAChR-ligand interactions at an atomic resolution.

MATERIALS AND METHODS

Homology modeling of the ECD structure for individual subunits of human nAChRs

The three dimensional models of nAChRs subunits were performed with a MODELLER v9.8 (38). Human α1 subunit was almost identical with the mouse α1 subunit. Human α3, β2, and β4 were also modeled. Sequence homology between human and mouse α1 is shown in Table 2. Cα RMSD between them was 0.458 Å. Cα RMSD of human α3, β2, and β4 compared with 2QC1 was 0.682 Å, 0.205 Å, and 0.258 Å, respectively. The results indicated that our models were proper. The dimeric and pentameric structures with GIC were generated by following procedures: (a) the modeled monomeric subunit was aligned to the corresponding monomer unit of 2C9T, (b) substituted to it with corresponding position, and (c) α-conotoxin ImI in 2C9T was substituted to GIC with the same procedures.

Supporting Information

Details of the molecular dynamics simulations and the methods of trajectory analysis are available free of charge at http://www.bmbreport.org.

REFERENCES

1. Corringer, P. J., Novere, N. L. and Changeux, J. P. (2000) Nicotinic receptors at the amino acid level. *Annu. Rev. Pharmacol. Toxicol.* **40**, 431-458.
2. Arias, H. R. (2000) Localization of agonist and competitive antagonist binding sites on nicotinic acetylcholine receptors. *Neurochem. Int.* **36**, 595-645.
3. Paterson, D. and Nordberg, A. (2000) Neuronal nicotinic receptors in the human brain. *Prog. Neurobiol.* **61**, 75-111.
4. Myers, R. A., Cruz, L. J., Rivier, J. E. and Olivera, B. M. (1993) Conus peptides as chemical probes for receptors and ion channels. *Chem. Rev.* **93**, 1923-1936.
5. Hu, S.-H., Gehrmann, J., Alewood, P. F., Craik, D. J. and Martin, J. L. (1997) Crystal structure at 1.1 Å resolution of α-conotoxin PnIB: Comparison with α-conotoxins PnIA and GI. *Biochemistry* **36,** 11323-11330.
6. McIntosh, J. M., Dowell, C., Watkins, M., Garrett, J. E., Yoshikami, D. and Olivera, B. M. (2002) α-Conotoxin GIC from Conus geographus, a novel peptide antagonist of nicotinic acetylcholine receptors. *J. Biol. Chem.* **277**, 33610-33615.
7. Martinez, J. S., Olivera, B. M., Gray, W. R., Craig, A. G., Groebe, D. R., Abramson, S. N. and McIntosh, J. M. (1995). α-Conotoxin EI, A new nicotinic acetylcholine receptor antagonist with novel selectivity. *Biochemistry* **34**, 14519-14526.
8. López-Vera, E., Aguilar, M. B., Schiavon, E., Marinzi, C., Ortiz, E., Restano Cassulini, R., Batista, C. V. F., Possani, L. D., Heimer de la Cotera, E. P., Peri, F., Becerril, B. and Wanke, E. (2007) Novel α-conotoxins from Conus spurius and the α-conotoxin EI share high-affinity potentiation and low-affinity inhibition of nicotinic acetylcholine receptors. *FEBS J.* **274**, 3972-3985.
9. McIntosh, J. M., Plazas, P. V., Watkins, M., Gomez-Casati, M. E., Olivera, B. M. and Elgoyhen, A. B. (2005) A novel α-conotoxin, PeIA, cloned from Conus pergrandis, discriminates between rat α9α10 and α7 nicotinic cholinergic receptors. *J. Biol. Chem.* **280**, 30107-30112.
10. López-Vera, E., Jacobsen, R. B., Ellison, M., Olivera, B. M. and Teichert, R. W. (2007) A novel alpha conotoxin (α-PIB) isolated from C. purpurascens is selective for skeletal muscle nicotinic acetylcholine receptors. *Toxicon.* **49**, 1193-1199.
11. Sandall, D. W., Satkunanathan, N., Keays, D. A., Polidano, M. A., Liping, X., Pham, V., Down, J. G., Khalil, Z., Livett, B. G. and Gayler, K. R. (2003) A novel α-conotoxin Identified by gene sequencing is active in suppressing the vascular response to selective stimulation of sensory nerves in vivo. *Biochemistry* **42**, 6904-6911.
12. Cartier, G. E., Yoshikami, D., Gray, W. R., Luo, S., Olivera, B. M. and McIntosh, J. M. (1996) A new α-conotoxin which targets 32 nicotinic acetylcholine receptors. *J. Biol. Chem.* **271**, 7522-7528.
13. Gray, W. R., Luque, A., Olivera, B. M., Barrett, J. and Cruz, L. J. (1981) Peptide toxins from Conus geographus venom. *J. Biol. Chem.* **256**, 4734-4740.
14. Chi, S.-W., Kim, D.-H., Olivera, B. M., McIntosh, J. M. and Han, K.-H. (2004) Solution conformation of alpha-conotoxin GIC, a novel potent antagonist of α3β2 nicotinic acetylcholine receptors. *Biochem. J.* **380**, 347-352.
15. Chi, S.-W., Lee, S.-H., Kim, D.-H., Kim, J.-S., Olivera, B. M., McIntosh, J. M. and Han, K.-H. (2005) Solution structure of α-conotoxin PIA, a novel antagonist of α6 subunit containing nicotinic acetylcholine receptors. *Biochem. Biophys. Res. Commun.* **338**, 1990-1997.
16. Chi, S.-W., Park, K.-H., Suk, J.-E., Olivera, B. M., McIntosh, J. M. and Han, K.-H. (2003) Solution conformation of αA-conotoxin EIVA, a potent neuromuscular nicotinic acetylcholine receptor antagonist from *Conus ermineus*. *J. Biol. Chem.* **278**, 42208-42213.
17. Han, K.-H., Hwang, K.-J., Kim, S.-M., Kim, S.-K., Gray, W. R., Olivera, B. M., Rivier, J. and Shon, K.-J. (1997) NMR structure determination of a novel conotoxin, [Pro 7,13] αA-conotoxin PIVA. *Biochemistry* **36**, 1669-1677.

18. Hu, S.-H., Loughnan, M., Miller, R., Weeks, C. M., Blessing, R. H., Alewood, P. F., Lewis, R. J. and Martin, J. L. (1998) The 1.1 Å resolution crystal structure of [Tyr15]EpI, a novel α-conotoxin from *Conus episcopatus*, solved by direct methods. *Biochemistry* **37**, 11425-11433.

19. Park, K.-H., Suk, J.-E., Jacobsen, R., Gray, W. R., McIntosh, J. M. and Han, K.-H. (2001) Solution conformation of α-conotoxin EI, a neuromuscular toxin specific for the α1/δ subunit interface of torpedo nicotinic acetylcholine receptor. *J. Biol. Chem.* **276**, 49028-49033.

20. Shon, K.-J., Koerber, S. C., Rivier, J. E., Olivera, B. M. and McIntosh, J. M. (1997) Three-dimensional solution structure of α-conotoxin MII, an α3β2 neuronal nicotinic acetylcholine receptor-targeted ligand. *Biochemistry* **36**, 15693-15700.

21. Cho, J.-H., Mok, K. H., Olivera, B. M., McIntosh, J. M., Park, K.-H. and Han, K.-H. (2000) Nuclear magnetic resonance solution conformation of α-conotoxin AuIB, an α3β4 subtype-selective neuronal nicotinic acetylcholine receptor antagonist. *J. Biol. Chem.* **275**, 8680-8685.

22. Brejc, K., van Dijk, W. J., Klaassen, R. V., Schuurmans, M., van der Oost, J., Smit, A. B. and Sixma, T. K. (2001) Crystal structure of an ACh-binding protein reveals the ligand-binding domain of nicotinic receptors. *Nature* **411**, 269-276.

23. Celie, P. H. N., Kasheverov, I. E., Mordvintsev, D. Y., Hogg, R. C., van Nierop, P., van Elk, R., van Rossum-Fikkert, S. E., Zhmak, M. N., Bertrand, D., Tsetlin, V., Sixma, T. K. and Smit, A. B. (2005) Crystal structure of nicotinic acetylcholine receptor homolog AChBP in complex with an α-conotoxin PnIA variant. *Nat. Struct. Mol. Biol.* **12**, 582-588.

24. Dellisanti, C. D., Yao, Y., Stroud, J. C., Wang, Z.-Z. and Chen, L. (2007) Crystal structure of the extracellular domain of nAChR α1 bound to α-bungarotoxin at 1.94 Å resolution. *Nat. Neurosci.* **10**, 953-962.

25. Ulens, C., Hogg, R. C., Celie, P. H., Bertrand, D., Tsetlin, V., Smit, A. B. and Sixma, T. K. (2006) Structural determinants of selective α-conotoxin binding to a nicotinic acetylcholine receptor homolog AChBP. *Proc. Natl. Acad. Sci. U.S.A* **103**, 3615-3620.

26. Grant, M. A., Gentile, L. N., Shi, Q.-L., Pellegrini, M. and Hawrot, E. (1999) Expression and spectroscopic analysis of soluble nicotinic acetylcholine receptor fragments derived from the extracellular domain of the α-subunit. *Biochemistry* **38**, 10730-10742.

27. Bren, N. and Sine, S. M. (2000) Hydrophobic pairwise interactions stabilize α-conotoxin MI in the muscle acetylcholine receptor binding site. *J. Biol. Chem.* **275**, 12692-12700.

28. Chiara, D. C., Xie, Y. and Cohen, J. B. (1999) Structure of the agonist-binding sites of the torpedo nicotinic acetylcholine receptor: Affinity-labeling and mutational analyses identify γTyr-111/δArg-113 as antagonist affinity determinants. *Biochemistry* **38**, 6689-6698.

29. Quiram, P. A., McIntosh, J. M. and Sine, S. M. (2000) Pairwise interactions between neuronal α7acetylcholine receptors and α-conotoxin PnIB. *J. Biol. Chem.* **275**, 4889-4896.

30. Sugiyama, N., Marchot, P., Kawanishi, C., Osaka, H., Molles, B., Sine, S. M. and Taylor, P. (1998) Residues at the subunit interfaces of the nicotinic acetylcholine receptor that contribute to α-conotoxin M1 binding. *Mol. Pharmacol.* **53**, 787-794.

31. Dutertre, S., Nicke, A., Tyndall, J. D. A. and Lewis, R. J. (2004) Determination of α-conotoxin binding modes on neuronal nicotinic acetylcholine receptors. *J. Mol. Recogn.* **17**, 339-347.

32. Hansen, S. B., Sulzenbacher, G., Huxford, T., Marchot, P., Taylor, P. and Bourne, Y. (2005) Structures of Aplysia AChBP complexes with nicotinic agonists and antagonists reveal distinctive binding interfaces and conformations. *EMBO J.* **24**, 3635-3646.

33. Bourne, Y., Talley, T. T., Hansen, S. B., Taylor, P. and Marchot, P. (2005) Crystal structure of a Cbtx-AChBP complex reveals essential interactions between snake α-neurotoxins and nicotinic receptors. *EMBO J.* **24**, 1512-1522.

34. Fraenkel, Y., Shalev, D. E., Gershoni, J. M. and Navon, G. (1996) Nuclear magnetic resonance (NMR) analysis of ligand receptor interactions: the cholinergic system-a model. *CRC, Crit. Rev. Biochem. Mol. Biol.* **31**, 273-301.

35. Luo, S., Nguyen, T. A., Cartier, G. E., Olivera, B. M., Yoshikami, D. and McIntosh, J. M. (1999) Single-residue alteration in α-conotoxin PnIA switches its nAChR subtype selectivity. *Biochemistry* **38**, 14542-14548.

36. McIntosh, J. M., Azam, L., Staheli, S., Dowell, C., Lindstrom, J. M., Kuryatov, A., Garrett, J. E., Marks, M. J. and Whiteaker, P. (2004) Analogs of α-conotoxin MII are selective for α6-containing nicotinic acetylcholine receptors. *Mol. Pharmacol.* **65**, 944-952.

37. Mok, K. H. and Han, K.-H. (1999) NMR solution conformation of an antitoxic analogue of α-conotoxin GI: identification of a common nicotinic acetylcholine receptor α1-subunit binding surface for small ligands and α-conotoxins. *Biochemistry* **38**, 11895-11904.

38. Martí-Renom, M. A., Stuart, A. C., Fiser, A., Sánchez, R., Melo, F. and Šali, A. (2000) Comparative protein structure modeling of genes and genomes. *Annu. Rev. Biophys. Biomol. Struct.* **29**, 291-325.

39. Homer, N., Merriman, B. and Nelson, S. (2009) Local alignment of two-base encoded DNA sequence. *BMC Bioinformatics* **10**, 175.

40. Dutertre, S., Ulens, C., Buttner, R., Fish, A., van Elk, R., Kendel, Y., Hopping, G., Alewood, P. F., Schroeder, C., Nicke, A., Smit, A. B., Sixma, T. K. and Lewis, R. J. (2007) AChBP-targeted α-conotoxin correlates distinct binding orientations with nAChR subtype selectivity. *EMBO J.* **26**, 3858-3867.

41. Le Novére, N., Grutter, T. and Changeux, J.-P. (2002) Models of the extracellular domain of the nicotinic receptors and of agonist- and Ca^{2+}-binding sites. *Proc. Natl. Acad. Sci. U.S.A* **99**, 3210-3215.